Orotate Phosphoribosyltransferase and Hypoxanthine/Guanine Phosphoribosyltransferase from Yeast: Nuclear Magnetic Relaxation Studies of the Structures of Enzyme-Bound Phosphoribosyl 1-Pyrophosphate†

Danyal B. Syed,‡ Rosalyn S. Strauss, and Donald L. Sloan*

Department of Chemistry and Ph.D. Program in Biochemistry, City College of The City University of New York, New York, New York 10031

Received July 11, 1986; Revised Manuscript Received September 29, 1986

ABSTRACT: Nuclear magnetic relaxation rate measurements have been performed on the protons and phosphorus atoms of phosphoribosyl 1-pyrophosphate (PRibPP) in the presence and absence of paramagnetic chromium(III), cobalt(II), and manganese(II) ions. The longitudinal relaxation rates were then used to calculate interatomic distances between the magnetic nuclei and these paramagnetic probes, from which was devised a conformation of the PRibPP–metal ion complex in solution. Thereafter, the experiments were accomplished in the presence of Mn(II) and a series of orotate phosphoribosyltransferase (OPRTase) and hypoxanthine/guanine phosphoribosyltransferase (HGPRTase) concentrations, and from these data were estimated the distances between Mn(II) and the PRibPP nuclei at the active sites of these two enzymes from yeast. Comparisons between the Mn(II)–PRibPP conformation in solution and this structure at the active sites of OPRTase and HGPRTase revealed that the metal ion remained coordinated with the pyrophosphate group of PRibPP in all instances, whereas the overall distances between the ribose ring and Mn(II) at the enzyme active sites were approximately 1 Å further from the metal ion. Model building studies also revealed that the 5′-phosphate group of PRibPP is positioned directly over the ribose ring in solution and at the OPRTase and HGPRTase active sites and may protect the 1′-carbon of PRibPP against on-line displacements of pyrophosphate under these conditions, where the PRibPP-to-Mn(II) concentration ratio is greater than 2000. Additional metal ions must be present at both of these enzyme active sites to provide optimal activity [Victor, J., Leo-Mensah, A., & Sloan, D. L. (1979) *Biochemistry 18*, 3597–3604; Ali, L. Z., & Sloan, D. L. (1983) *Biochemistry 22*, 3419–3424], and we speculate that these additional metal ions may reposition the 5′-phosphate group and enhance the reactivity of the 1′-carbon as a result.

Both orotate phosphoribosyltransferase (OPRTase)[1] and hypoxanthine/guanine phosphoribosyltransferase (HGPRTase) have been purified to homogeneity from *Saccharomyces cerevisiae* (Umezu et al., 1970; Schmidt et al., 1979). The kinetic mechanisms by which these enzymes proceed (eq 1 and 2) have been determined (Victor et al., 1979a; Ali & Sloan, 1982), as have the mechanisms through which divalent metal ions activate these phosphoribosyl group transfers (Victor et al., 1979b; Ali & Sloan, 1983). As shown in eq 1, OPRTase catalyzes the formation of orotidine monophosphate (OMP) via a ping-pong Bi-Bi kinetic mechanism under optimal conditions (Victor et al., 1979a) and utilizes a metal ion–PRibPP complex as substrate. In contrast (eq 2), the HGPRTase-catalyzed formation of either guanosine 5′-monophosphate (GMP) or inosine 5′-monophosphate (IMP) proceeds through the use of an ordered Bi-Bi kinetic mechanism (Ali & Sloan, 1982) and a metal ion–PRibPP complex. In addition, the active form of OPRTase can be either an apoenzyme or an enzyme–metal ion complex [either Mn(II) or Mg(II); Victor et al., 1979b], whereas the active form of HGPRTase requires a divalent metal ion (a fairly broad metal ion specificity; Ali & Sloan, 1983, 1986).

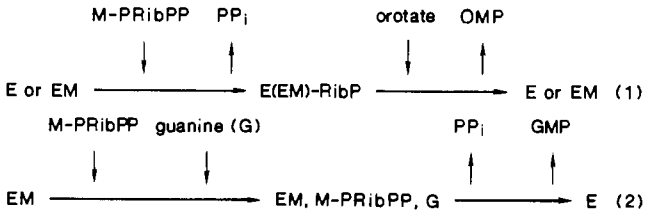

Our observation, that significant differences exist in the kinetic properties of the OPRTase- and HGPRTase-catalyzed reactions, prompted us to initiate NMR studies of the geometry of these enzyme–PRibPP complexes, with Mn(II) as a paramagnetic probe, in order to determine if each enzyme would bind their common substrate in a unique conformation. Measurements of the effects of paramagnetic metal ions on substrate proton and phosphorus magnetic relaxation rates are now considered to be standard procedures for evaluating enzyme-bound reactant conformations and juxtapositions (Mildvan & Cohn, 1966, 1970; Sloan et al., 1975; Mildvan & Gupta, 1978; Jarori et al., 1985). A preliminary account of a portion of this work has been presented (Syed et al., 1985).

† This work was accomplished with support from NIH Grants AM-20183 and RR-08168 (MBRS). Further support was provided by the CUNY Research Foundation. The relaxation rate measurements were performed at 400 MHz at the CUNY NMR Facility, which was established with NSF Grant PCM-8111745. Additional NMR instrument time at 220 MHz was provided by Dr. David Cowburn and the NMR Consortium of Rockefeller University.

* Author to whom correspondence should be addressed.

‡ Present address: Clinical Chemistry Division, Hartford Hospital and Medical Center, Hartford, CT 06101.

[1] Abbreviations: HGPRTase, hypoxanthine/guanine phosphoribosyltransferase; OPRTase, orotate phosphoribosyltransferase; PRibPP, phosphoribosyl 1-pyrophosphate; $1/T_1$, longitudinal relaxation rate; $1/T_2$, transverse relaxation rate; OMP, orotidine 5′-monophosphate; GMP, guanosine 5′-monophosphate; IMP, inosine 5′-monophosphate; Tris, tris(hydroxymethyl)aminomethane; NOE, nuclear Overhauser effect.

0006-2960/87/0426-1051$01.50/0

Experimental Procedures

Materials. The following reagents were obtained from Sigma Chemical Co. (St. Louis): hypoxanthine, guanine, orotic acid, and PRibPP (tetrasodium salt). The chloride salts of divalent manganese, magnesium, and cobalt and of trivalent chromium were Baker Analytical reagents. Bio-Rad Laboratories provided Cellex-D, Chelex-100, Dowex-AG 50W X-4 (protonated form), and Dowex-AG 1 X-4 (chloride form), whereas Pharmacia provided AH-Sepharose-4B and Sephadex G-10. All other reagents were analytical grade. Distilled water was further purified and deionized (to a conductivity reading of 18) with a Gelman Water-I Purifier.

Enzyme Purifications from Saccharomyces cerevisiae. HGPRTase was purified to apparent electrophoretic homogeneity from 50 lb of Budweiser brand baker's yeast (Valente Yeast Inc., Flushing, NY) according to the procedure of Ali and Sloan (1982). A single preparation of this enzyme (specific activity 1300 units/mg)[2] was employed in the NMR studies. OPRTase was purified from this same source according to the procedures described by Umezu et al. (1971) and by Victor et al. (1979a,b). Three preparations from 60 lb of yeast were employed in the NMR studies, all of which were at least 95% pure as determined by gel electrophoresis (specific activity range 125–175 units/mg).

Assay Procedures. The enzyme-catalyzed formation of OMP was monitored spectroscopically with a Cary-15 recording spectrophotometer by observing the disappearance of orotate absorbance at 295 nm (Umezu et al., 1971). The final concentrations of reactants in 1 mL of assay solution were 100 μM PRibPP, 2 mM $MgCl_2$, 150 μM orotate, and 20 mM Tris-HCl buffer (pH 8). The enzymatic formation of GMP was monitored initially with a spectroscopic procedure, during which the increase of GMP absorbance at 245 nm was observed (Hill, 1979) in assay solutions, assembled as described by Flaks (1963).

During the final stages of purification and during the NMR experiments, an assay that employed high-performance liquid chromatography was used to follow HGPRTase activity (Ali & Sloan, 1982; Sloan, 1984). The assay solution consisted of 100 μM hypoxanthine, 200 μM PRibPP, and 1 mM $MgCl_2$ in 20 mM ethanolamine (pH 8).

NMR Sample Preparation. All glassware and NMR tubes were allowed to stand for 5 h in 1 N HNO_3 and then were rinsed thoroughly with high-conductivity water. All of the PRibPP and enzyme solutions were dissolved in metal-free Tris-HCl and then eluted through Chelex-100 minicolumns. The extent of removal of Mg(II) and Mn(II) in these solutions was examined kinetically by observing the absence of either HGPRTase or OPRTase activities, without prior addition of these metal ions to the assay solutions. Prior to the ^1H NMR experiments, vacuum dialysis (Slater et al., 1972) was employed to place the samples into D_2O.

Magnetic Relaxation Measurements. The longitudinal relaxation times (T_1) of the protons and phosphorus atoms of PRibPP were measured by an inversion recovery method at 161.8 (phosphorus) and 400 (hydrogen) MHz, using the JEOL GX-400 Fourier transform NMR spectrometer at the CUNY NMR Facility (at Hunter College). Additional experiments were performed at Rockefeller University on a Varian HFX-220 spectrometer. The temperature was maintained at 19 °C throughout these experiments.

[2] Units of HGPRTase activity are defined as micromoles of GMP (or IMP) formed per minute, whereas units of OPRTase activity are defined as micromoles of OMP formed per minute.

The value of $1/T_1$ (the relaxation rate) for each individual resonance was determined through the use of three plotting devices: (1) A null-point method (Mildvan & Engle, 1972) was used, where the time (t) between the 180° and 90° pulses that leads to the minimization of M_z (the magnetization in the z direction of a rotating coordinate frame) is related to T_1 through the relationship

$$t_{null} = T_1 \ln [(M - M_t)/M] = T_1 \ln 2 \quad (3)$$

where M is this magnetization when t is equal to infinity. (2) Two arrangements of the Bloch equation (Mildvan & Cohn, 1970), which define T_1 from the y intercept of a plot of ln ($M - M_t$) with t (eq 4) and from the slope of a plot of $-\ln [(M - M_t)/2M]$ with t (eq 5), were also employed. (3) The best

$$\ln (M - M_t) = \ln (M - M_0)e^{-t/T_1} \quad (4)$$

$$-\ln [(M - M_t)/2M] = t/T_1 \quad (5)$$

fit computer procedure of Kowalewski (1977) also was adapted for use in our laboratory by Robert W. Ashton. The calculated values of each relaxation rate, obtained by these three methods, were then averaged and used to calculate additional parameters, including interatomic distances. Transverse relaxation rates were estimated from the line widths of the individual resonances at half-height (Mildvan & Engle, 1972).

Calculation of Correlation Times and Distances. Paramagnetic effects on the longitudinal ($1/T_{1p}$) and transverse ($1/T_{2p}$) relaxation rates were calculated by subtracting the $1/T_1$ and $1/T_2$ values of appropriate diamagnetic samples from those rates measured on samples containing various paramagnetic ions [Mn(II), Co(II), or Cr(III)], by using published procedures (Mildvan & Cohn, 1970; Mildvan & Engle, 1972; Mildvan & Gupta, 1978). The diamagnetic corrections for the binary Mn(II)–PRibPP complex were made by using the PRibPP relaxation rates in the absence of any metal ion. For the ternary OPRTase–Mn(II)–PRibPP and HGPRTase–Mn(II)–PRibPP complexes, these corrections were made by using nonmetallic OPRTase–PRibPP and HGPRTase–PRibPP solutions. All of the calculated $1/T_{1p}$ values were normalized (Luz & Meiboom, 1964) with a concentration ratio (f) equal to [Mn(II)]/[PRibPP] and were determined (vide infra) not to represent ligand-exchange rates (the fast-exchange condition). Distances (r) from the paramagnetic ion to the magnetic nuclei of PRibPP were calculated by using the dipolar term of the Solomon–Bloembergen equation (eq 6), in

$$r = C[fT_{1p}[f(t_c)]]^{1/6} \quad (6)$$

which the parameter C is a collection of constants well-defined for each paramagnetic center (Solomon, 1955; Bloembergen, 1957). The correction function $[f(t_c)]$ is related to the correlation time for the dipolar interaction t_c by eq 7. An

$$f(t_c) = 3t_c/(1 + \omega_i^2 t_c^2) + 7t_c/(1 + \omega_S^2 t_c^2) \quad (7)$$

evaluation of $f(t_c)$ cannot be accomplished from measurements of $1/T_{1p}$ at different frequencies in the range of 200–500 MHz. However, estimates of t_c can be calculated from T_{1p}/T_{2p} ratios (Ray & Mildvan, 1970) and T_1/T_2 ratios (Ferrin & Mildvan, 1985) for use in the distance calculations.

Results

Measurements of Magnetic Relaxation Rates of the Protons of PRibPP. The longitudinal and transverse relaxation rates of the five resolved protons of PRibPP (Figure 1A) were measured at 400 and 220 MHz at the CUNY NMR Consortium Facility and Rockefeller University, respectively. The following ppm assignments of resonances (400 MHz) were

Table I: Effect of Paramagnetic Metal Ions on Longitudinal Relaxation Rates of the Protons of PRibPP ($1/fT_{1p}$ in s^{-1}) at 400 and 220 MHz and Calculated Distances (r in Å) between the Metal Ion and These Protons[a]

exptl conditions	parameter	proton 1	2	3	4	5
220 MHz, 100 mM PRibPP						
10 μM Mn(II)	$1/fT_{1p}$	10800	6400	5200	2400	2600
	r	4.5 ± 0.5	4.9 ± 0.3	5.1 ± 0.3	5.7 ± 0.5	6.0 ± 0.5
400 MHz, 10 mM PRibPP						
20 μM Mn(II)	$1/fT_{1p}$	4612	2504	563	544	989
	r	5.0 ± 0.5	5.7 ± 0.2	7.3 ± 0.4	7.3 ± 0.3	6.4 ± 0.2
20 μM Co(II)	$1/fT_{1p}$	297	169	86	42	126
	r	4.8 ± 0.9	5.4 ± 0.9	7.0 ± 1.5	7.0 ± 1.2	5.8 ± 1.0
20 μM Cr(III)	$1/fT_{1p}$	102	62	42	61	225
	r	8.4 ± 0.9	9.6 ± 1.0	9.3 ± 1.0	7.8 ± 0.8	7.8 ± 0.8

[a] The fT_{1p} values were calculated from the average $1/T_1$ values obtained by three plotting methods for each proton as described under Experimental Procedures. $f(t_c)$ values for Mn(II), Co(II), and Cr(III) complexes in solution equal to 3×10^{-10}, 7×10^{-12}, and 4×10^{-10} s were employed in these calculations.

accomplished with reference to the Tris-HCl proton singlet (3.47 ppm) in the sample: 5.50 (1′-proton, H1), 4.14 (2′-proton, H2), 3.97 (3′-proton, H3), 3.90 (4′-proton, H4), and 3.60 (5′-proton, H5). The longitudinal relaxation rates ($1/T_1$) of these protons were measured, through the use of the three procedures described under Experimental Procedures, with a calculated average deviation of ±4%. The $1/T_2$ values, estimated from line width measurements of these resonances, were determined with a calculated average uncertainty of 20%. The average $1/T_1$ values, measured in the presence of several paramagnetic probes, were used to calculate the $1/T_{1p}$ and $1/fT_{1p}$ values listed in Table I. As shown in Table I, metal ion to nuclei distances can be calculated from the $1/fT_{1p}$ values by using $f(t_c)$ values of 3×10^{-10} (Sloan & Mildvan, 1976; Jarori et al., 1985), 7×10^{-12} (Gupta et al., 1976), and 3.9×10^{-10} (Peterson & Gupta, 1979) for Mn(II), Co(II), and Cr(III), respectively, and by using values for the collection of constants (C) of 812 (Tinkham et al., 1951), 900 (Luz & Meiboom, 1964), and 710 (Peterson & Gupta, 1979) for these metal ions, respectively. As expected, the values obtained at 220 MHz are analogous to those obtained at 400 MHz. The calculated Cr(III)-to-proton distances (7.8–9.6 Å) reveal that the exchange-inert Cr(III) does not coordinate any portion of the PRibPP molecule, whereas both the calculated Co(II)-to-proton and Mn(II)-to-proton distances confirm our suggestion (Victor et al., 1979b) that 1-to-1 coordination occurs between PRibPP and Co(II) and Mn(II) under these conditions. The calculated distances from the data accumulated at 400 MHz are the most reliable, since the high concentration (100 mM) of PRibPP employed in the studies at 220 MHz would not preclude Mn(II) from affecting the relaxation rates of molecules near to, but not coordinated to, the metal ion. Since we had observed earlier that Mn(II), but not Co(II), is an activator of both OPRTase and HGPRTase from yeast (Victor et al., 1979b; Ali & Sloan, 1983), and because the paramagnetic effect of Mn(II) on the PRibPP protons is by far the most efficient, we elected to initiate a study of the Mn(II) ion–PRibPP complex bound to these enzymes rather than the Co(II) complex. We determined further that neither of these two enzymatic activities would survive fully the time of experimentation with both paramagnetic ions, thus necessitating a choice.

Magnetic Relaxation Rate Measurements of the Protons of Enzyme-Bound PRibPP. We have observed that the $1/fT_{1p}$ values of the protons of PRibPP in the presence of either OPRTase or HGPRTase are proportional to the concentration (0–80 μM) of added Mn(II) and can therefore be used to calculate distances between the metal ion and the protons of the enzyme-bound PRibPP, once an appropriate t_c value is

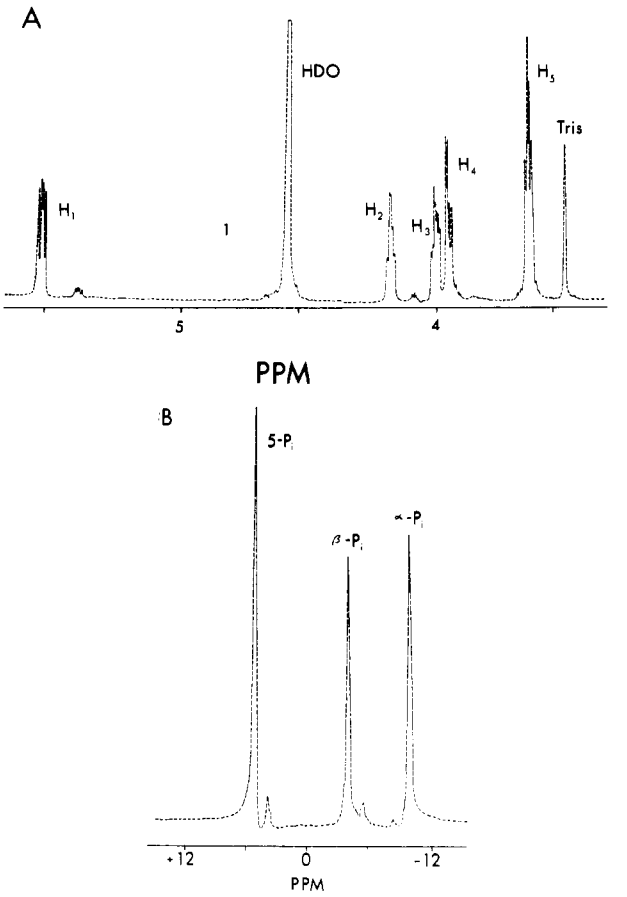

FIGURE 1: (A) ^1H NMR spectrum of PRibPP (10 mM) in 5 mM Tris, pH 8, at 400 MHz in 99.97% D_2O. The proton resonances, which were positioned relative to the Tris buffer singlet resonating at 3.47 ppm, are located at 5.50 (1′-H), 4.14 (2′-H), 3.97 (3′-H), 3.91 (4′-H), and 3.60 (5′-H) ppm. (B) The ^{31}P NMR spectrum of PRibPP (10 mM) in 5 mM Tris, pH 8, at 161.8 MHz in 50% D_2O. The broad band decoupled phosphorus resonances are positioned at 5.1 (5′-P_i), −4.4 (β-P_i), and −10.7 (α-P_i) ppm from the 85% orthophosphoric acid standard.

obtained and if the results can be extrapolated to an enzyme concentration where all of the metal ion resides at the PRibPP binding site. In this section we describe our measurements of the effect of Mn(II) on the $1/T_1$ values of the protons of PRibPP in the presence of increasing concentrations of OPRTase and HGPRTase and our calculation of the t_c values.

At 400 MHz, the order of the normalized paramagnetic effects of Mn(II) on the protons of PRibPP in the absence of enzyme is H1 > H2 > H5 = H3 = H4, and this order is maintained in the presence of 250 μM OPRTase (Table II).

Table II: Effects at 400 and 220 MHz of the Addition of Mn(II) on Longitudinal Relaxation Rates ($1/fT_{1p}$ in s^{-1}) of the Protons of PRibPP in the Presence of OPRTase and HGPRTase[a]

exptl conditions	parameter	proton 1	2	3	4	5
400 MHz, 10 mM PRibPP, 80 μM Mn(II)						
250 μM OPRTase	$1/fT_{1p}$	3720	2075	578	359	615
125 μM OPRTase	$1/fT_{1p}$	3795	2152	1435	539	1148
62.5 μM OPRTase	$1/fT_{1p}$	6900	2258	1608	1337	1518
infinite enzyme[b]	$1/fT_{1p}$	3160	1995	525	229	479
	r	5.5 ± 0.4	6.7 ± 0.6	8.0 ± 0.4	8.7 ± 0.8	8.2 ± 0.9
400 MHz, 10 mM PRibPP, 80 μM Mn(II)						
650 μM HGPRTase	$1/fT_{1p}$	3031	1411	746	323	238
330 μM HGPRTase	$1/fT_{1p}$	4169	2295	639	393	385
166 μM HGPRTase	$1/fT_{1p}$	4593	2884	694	460	756
infinite enzyme[b]	$1/fT_{1p}$	3600	1230	708	302	166
	r	5.2 ± 0.5	6.3 ± 0.7	7.5 ± 0.8	9.0 ± 0.8	9.5 ± 09
220 MHz, 10 mM PRibPP, 10 μM Mn(II)						
1000 μM OPRTase	$1/fT_{1p}$	3600	2800	1200	1200	1000
500 μM OPRTase	$1/fT_{1p}$	5000	3400	4000	4000	3600
250 μM OPRTase	$1/fT_{1p}$	15200	11000	9400	9400	5600
infinite enzyme[b]	$1/fT_{1p}$	3000	2100	800	800	420
	r	5.6 ± 0.7	6.7 ± 0.7	7.8 ± 0.8	7.8 ± 0.8	8.4 ± 0.9

[a] The evaluation of this parameter and the calculation of interatomic distances (r in Å) were accomplished as described in the text. [b] These values of $1/fT_{1p}$ were obtained by extrapolating plots of the log ($1/fT_{1p}$) vs. the reciprocal of the OPRTase concentration to infinite enzyme concentration as shown in Figure 2A, B.

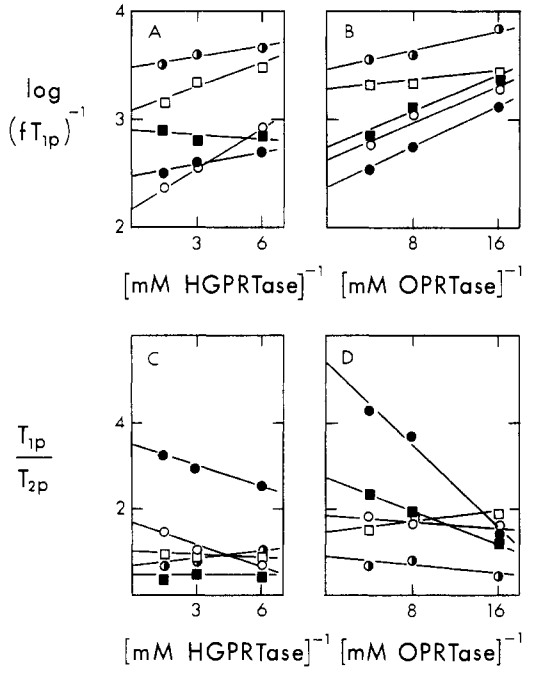

FIGURE 2: Plots of log ($1/fT_{1p}$) and T_{1p}/T_{2p} vs. 1/[E] for the protons of PRibPP in 5 mM Tris, pH 8, in the presence of 80 μM Mn(II). In all parts of the figure the 1′, 2′, 3′, 4′, and 5′ protons are represented by (◑), (□), (■), (●), and (○), respectively. (A) Plot of log ($1/fT_{1p}$) vs. 1/[HGPRTase]. (B) Plot of log ($1/fT_{1p}$) vs. 1/[OPRTase]. (C) Plot of T_{1p}/T_{2p} vs. 1/[HGPRTase]. (D) Plot of T_{1p}/T_{2p} vs. 1/[OPRTase].

Moreover, the order of effects also appears after the fT_{1p} values have been extrapolated to the "infinite enzyme" condition, a result that also was observed at 220 MHz (Figure 2B; Table II) even though the absolute values of these parameters have changed. These results suggest that the conformation of the OPRTase-bound Mn(II)–PRibPP may be similar to that found in solution. In contrast, the addition of 664 μM HGPRTase to the Mn(II)–PRibPP solution decreases significantly the effect of the metal ion on the 5′-proton (Figure 2A; Table II). The new order of paramagnetic effects is thus H1 > H2 > H3 = H4 > H5 for the HGPRTase solutions, including those obtained as a result of the extrapolation to infinite enzyme (Table II), suggesting that a slightly more significant conformational change has occurred as a result of the binding of Mn(II)–PRibPP to HGPRTase.

Table III: Calculated $f(t_c)$ Values, $\times 10^{10}$, for the Protons of Enzyme-Bound PRibPP[a]

enzyme complex	parameter	proton 1	2	3	4	5	av
PRibPP–OPRTase–Mn(II)	$f(t_c)$	2.6	5.0	5.5	4.1	5.9	4.6
PRibPP–HGPRTase–Mn(II)	$f(t_c)$	1.6	2.9	*b*	5.7	6.0	4.1

[a] The values were calculated by using extrapolation procedures described in the text and figure legends. [b] The extrapolated T_{1p}/T_{2p} ratio and each individually determined T_{1p}/T_{2p} ratio of the H3 proton in the HGPRTase-containing solutions were less than that dictated by the equations defined in Ray and Mildvan (1972).

In order to obtain additional information on the enzyme-bound conformations of PRibPP, we elected to calculate interatomic metal ion–ribose distances by making use of experimentally determined T_{1p}-to-T_{2p} ratios (Ray & Mildvan, 1975; Ferrin & Mildvan, 1985) to estimate the value of t_c. As shown in Figure 2C,D, just as the $1/fT_{1p}$ values were extrapolated to infinite enzyme, the values of T_{1p}/T_{2p} were so extrapolated, and these values were employed to calculate a series of t_c values. With this procedure, an order of magnitude range of t_c values (0.9×10^{-10}–6×10^{-10}) was determined for the OPRTase experiments at 400 MHz whereas a t_c value equal to 6.5×10^{-10} was obtained from the results at 220 MHz. A range of $f(t_c)$ values (2.6×10^{-10}–5.5×10^{-10}) was then calculated from both sets of data. The average $f(t_c)$ was determined to be $4.6 \times 10^{-10} \pm 1.7 \times 10^{-10}$. Table III also lists the values of $f(t_c)$ calculated for the HGPRTase results according to the T_{1p}/T_{2p} extrapolation procedure. A range of t_c values (0.6×10^{-10}–5.6×10^{-10}) was obtained from these data, and an average $f(t_c)$ was calculated to be $4.1 \times 10^{-10} \pm 1.8 \times 10^{-10}$. These average $f(t_c)$ values for the OPRTase and HGPRTase samples were then employed in the metal ion–PRibPP proton distance calculations (Table II), and the maximal and minimal values were used to evaluate the uncertainties in the distances (Table II).

Magnetic Relaxation Rates of the Phosphorus Atoms of PRibPP. The chemical shifts of the 5′-, α-, and β-phosphorus

Table IV: Effects of Addition of Mn(II) on Longitudinal Relaxation Rates ($1/fT_{1p}$ in s^{-1}) of the Phosphorus Atoms of PRibPP in the Presence of OPRTase and HGPRTase[a]

exptl conditions	parameter	phosphorus atom 5′-P_i	β-P_i	α-P_i
10 mM PRibPP, 4 μM Mn(II)				
no enzyme[b]	$1/fT_{1p} \times 10^{-3}$	4.7	17.6	15.5
	r	4.0 ± 0.2	3.3 ± 0.2	3.2 ± 0.2
241 μM OPRTase	$1/fT_{1p} \times 10^{-3}$	0.3	2.1	2.0
107 μM OPRTase	$1/fT_{1p}$	0.4	2.4	2.3
53.5 μM OPRTase	$1/fT_{1p}$	0.3	2.1	2.0
infinite enzyme[c]	$1/fT_{1p}$	0.4	2.1	2.5
	r	5.5 ± 0.2	4.3 ± 0.3	4.0 ± 0.2
541 μM HGPRTase	$1/fT_{1p} \times 10^{-3}$	1.5	9.7	3.2
271 μM HGPRTase	$1/fT_{1p}$	1.6	6.9	5.0
135 μM HGPRTase	$1/fT_{1p}$	5.0	11.9	7.1
infinite enzyme[d]	$1/fT_{1p}$	1.0	6.8	2.4
	r	5.2 ± 0.5	3.8 ± 0.3	4.0 ± 0.3

[a] The evaluation of this parameter and the calculation of interatomic distances (r in Å) were accomplished as described in the text. [b] The value of $f(t_c)$ employed in these calculations was 3×10^{-10}. [c] The value of $f(t_c)$ employed in these calculations was 4.3×10^{-10}. [d] The value of $f(t_c)$ employed in these calculations was 4.2×10^{-10}.

atoms of PRibPP were determined to be 5.1, −4.4, and −10.7 ppm with respect to 85% orthophosphoric acid (Figure 1B). The relative values of these shifts were similar to those observed for the 5-phosphate of ribose 5-phosphate in combination with the diphosphate portion of ADP in Tris buffer (pH 8), although the absolute values for the chemical shifts were slightly different from those reported by Smithers and O'Sullivan (1982) for PRibPP in a different buffer system. Increasing concentrations of Mn(II) increased proportionally the relaxation rates of the phosphate resonances of PRibPP, the greatest effect of which was felt by the β-phosphate group (Table IV). As shown in Figure 3, the values of $1/fT_{2p}$ are greater than the corresponding $1/fT_{1p}$ values by at least a factor of 10. These results indicate that the smaller $1/fT_{1p}$ values are not limited (Mildvan & Cohn, 1966; Nowak & Mildvan, 1972) or are only partially limited (Jarori et al., 1985) by the exchange rate of the metal ion from its ligands. To test whether the rate of PRibPP exchange made any contribution to the observed relaxation rate, the fastest measured relaxation rate (the $1/fT_{2p}$ of the α-phosphate) was employed as the lower limit of the value of $1/t_m$ (eq 8) in order

$$1/fT_{1p} = 1/(T_{1m} - t_m) \quad (8)$$

to estimate the maximum contribution of t_m to $1/fT_{1p}$. This calculated adjustment did not yield any significant change in the $1/fT_{1p}$ value, suggesting that the observed values of $1/fT_{1p}$ should be equal to their respective $1/T_{1m}$ values. Thus, as determined by this criterion, no adjustments in the Mn(II)-to-phosphorus distances were required. An analogous test was applied to the relaxation rates of the protons of PRibPP.

The metal ion to phosphorus distances of Mn(II)–PRibPP in solution were calculated by using an $f(t_c)$ value equal to 3×10^{-10}, which was determined from water proton longitudinal relaxation rate measurements of the Mn(II)–PRibPP complexation (Victor et al., 1979b). An analogous $f(t_c)$ value had been employed to evaluate Mn(II)–ATP distances in solution (Sloan & Mildvan, 1976; Jarori et al., 1985). These calculations reveal that, at a PRibPP-to-Mn(II) concentration ratio of 2500, the metal ion is coordinated directly to both the α- (r = 3.2 Å) and the β- (r = 3.3 Å) phosphate oxygen atoms of the pyrophosphate group. Interestingly, the position of the 5′-phosphate group is also near to the metal ion (4 ± 0.2 Å), although direct coordination is not indicated by this calculated distance (Sundaralingam, 1969).

The phosphorus relaxation rates were then obtained for PRibPP in the presence of increasing concentrations of both

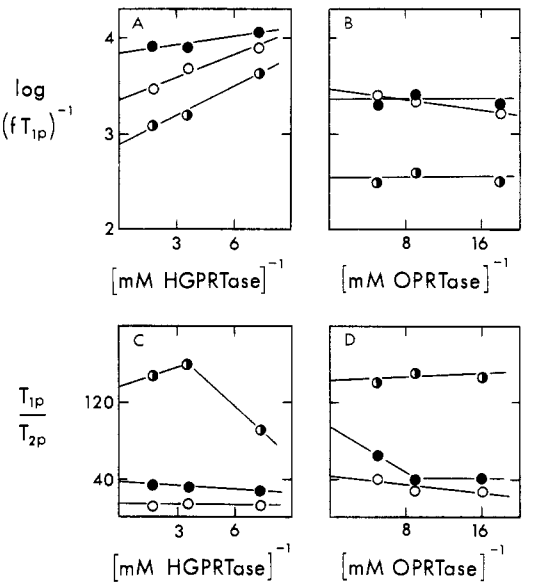

FIGURE 3: Plots of log $(1/fT_{1p})$ and T_{1p}/T_{2p} vs. $1/[E]$ for the phosphorus atoms of PRibPP in 5 mM Tris, pH 8, in the presence of 4 μM Mn(II). In all parts of the figure the 5′, β, and α resonances are represented by (◑), (○), and (●), respectively. (A) Plot of log $(1/fT_{1p})$ vs. 1/[HGPRTase]. (B) Plot of log $(1/fT_{1p})$ vs. 1/[OPRTase]. (C) Plot of T_{1p}/T_{2p} vs. 1/[HGPRTase]. (D) Plot of T_{1p}/T_{2p} vs. 1/[OPRTase].

OPRTase and HGPRTase. As shown in Table IV, the experimentally determined $1/fT_{1p}$ values at three different concentrations of each enzyme were extrapolated to infinite enzyme concentration (Figure 3A,B). These extrapolations resulted in a significant difference in the fT_{1p} value obtained at the highest HGPRTase concentration, but the extrapolated fT_{1p} was equivalent to this value determined for the highest OPRTase concentration, perhaps because all of the 4 μM Mn(II)–PRibPP is bound to OPRTase in all of the experiments. For each nuclei, the largest observed paramagnetic effect on the transverse relaxation rate is more than 10-fold greater than the observed values of $1/T_{1p}$, indicating, as stated previously, that $1/fT_{1p}$ is equivalent to $1/T_{1m}$ (eq 8). Once again the ratio of T_{1p} to T_{2p} of each nucleus was employed to evaluate $f(t_c)$. As listed in Table V and as illustrated in Figure 3C,D, the extrapolated phosphorus T_{1p}/T_{2p} values were determined with less precision than those evaluated for the PRibPP protons. However, the average $f(t_c)$ values (4×10^{-10} for OPRTase and 4.5×10^{-10} for HGPRTase) are analogous

Table V: Calculated $f(t_c)$ Values, $\times 10^{10}$, for the Phosphorus Atoms of Enzyme-Bound PRibPP[a]

enzyme complex	parameter	phosphorus 5′-P_i	β-P_i	α-P_i	av
PRibPP–OPRTase–Mn(II)	$f(t_c)$	2.3	5.3	4.5	4.0
PRibPP–HGPRTase–Mn(II)	$f(t_c)$	2.2	7.5	3.9	4.5

[a] The values were calculated by using extrapolation procedures described in the text and figure legends.

to those values calculated from the proton data. By use of these values, the Mn(II)-to-5′-phosphate distances for the OPRTase- and HGPRTase-bound PRibPP were calculated to be 5.5 ± 0.7 and 5.0 ± 0.5 Å, respectively. In contrast, the Mn(II)-to-pyrophosphate α-phosphorus distances were calculated to be 4.0 ± 0.3 Å for both enzyme complexes, whereas the β-phosphorus was calculated to be 4.0 ± 0.3 Å from the metal ion at the OPRTase active site and 3.8 ± 0.3 Å from this ion at the HGPRTase site. It has been established that the Mn(II)-to-phosphorus distance associated with an inner-sphere monodentate complex (for tetrahedral phosphate) is 3.2 ± 0.2 Å (Mildvan & Grisham, 1974; Mildvan et al., 1973). Thus, values closer to 4 Å require an alternate explanation. Several possibilities come to mind. (1) The pyrophosphate group may no longer contain tetrahedral phosphorus at these enzyme active sites (metal ion to pentacoordinate phosphate distances are approximately equal to 4 Å). (2) The Mn(II)-to-phosphate distances represent an average of coordinated and uncoordinated forms of PRibPP at the enzyme binding sites. (3) There may exist a partial contribution to T_{1p} from t_m so that direct coordination is obscured [partial exchange limitation as described by Rao (1984) that cannot be disclosed from the relative value of the T_{1p}/T_{2p} ratios]. These kinds of exchange limitations can be delineated by repeating the relaxation rate measurements in the presence of a second paramagnetic probe (Jarori et al., 1985), such as Co(II). We intend to carry out these experiments with Co(II), once additional preparations of OPRTase and HGPRTase are obtained.

Analysis of the Conformation of Mn(II)–PRibPP. Model structures of PRibPP were constructed on the basis of the eight metal ion–proton and –phosphorus distances listed in Tables I and IV for the 1:1 Mn(II) complex in solution. Although a single conformation cannot be identified from this number of distances, a conformation that fits these distances and exhibits a 2′-*endo*-ribose conformation, a gauche–gauche positioning of the 5′-phosphate, and minimal eclipsing for the pyrophosphate oxygen atoms can be constructed and is shown in Figure 4. The limitations on the model were that nonbonding distances must exceed the sum of the assumed atomic van der Waals radii (1.2 Å for hydrogen, 1.4 Å for carbon and oxygen, 1.7 Å for phosphorus). A position for the 5′-phosphate was found (Figure 4) that was consistent with the calculated distances and minimized the van der Waals overlap with the atoms of the ribofuranose ring. Space-filling models (not shown) also were constructed and confirmed that it is possible to locate the 5′-phosphate group near to the metal ion and above the ribose ring. As shown in Figure 4, the position of Mn(II), with respect to the phosphate and pyrophosphate groups of PRibPP, is similar to the relative positions of Mn(II) and the triphosphate group of ATP in solution (Sloan & Mildvan, 1976). The time-dependent nuclear Overhauser effect measurements, under way currently with 1:1 Mg-(II)–PRibPP, should define the metal ion–PRibPP ligation in solution with greater precision.

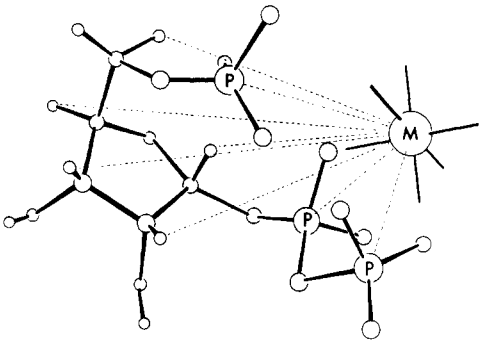

FIGURE 4: Model of structure of the Mn(II)–PRibPP complex consistent with calculated metal ion to PRibPP nuclear distances (dotted lines) determined from longitudinal magnetic relaxation rate measurements. The structural features constructed into the model were a 2′-*endo*-ribose puckered conformation, a gauche–gauche conformation for the 5′-phosphate, and a minimal eclipsing of the pyrophosphate oxygen atoms.

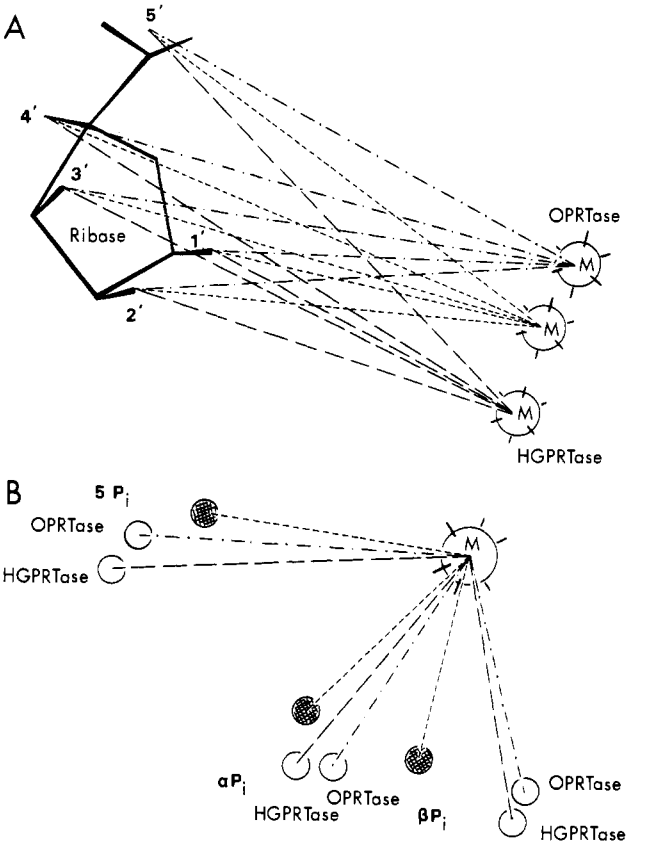

FIGURE 5: Comparisons of structural features of models constructed for Mn(II)–PRibPP, Mn(II)–PRibPP–HGPRTase, and Mn(II)–PRibPP–OPRTase on the basis of distances presented in Tables I, II, and IV. (A) Comparison of the position of the Mn ion with respect to the ribose ring on the basis of the calculated Mn(II)-to-PRibPP proton distances. The ribose portion of each model was superimposed for this comparison. (B) Comparison of the position of the phosphorus atoms of each structure with respect to the Mn ion on the basis of the calculated Mn(II)-to-PRibPP phosphorus atom distances. The positions of Mn(II) were superimposed for this comparison.

Models for the OPRTase-bound and HGPRTase-bound PRibPP conformations were constructed with the same assumptions used to define the solution M(II)-PRibPP conformation. A comparison of the three models is illustrated in Figure 5. As shown in Figure 5A, by overlapping the ribose rings of each model, the relative position of the Mn(II) is defined. These proton distances suggest that the metal ion is positioned sufficiently close to the pyrophosphate group in

all three models for direct coordination to occur. As shown in Figure 5B, the positions of the phosphorus atoms of PRibPP bound to both OPRTase and HGPRTase are similar. Once again the relative distances suggest that substantial percentages of PRibPP molecules bound to OPRTase and HGPRTase are coordinated to enzyme-bound metal ions, and we believe that NOE experments (Clore & Gronenborn, 1983) may define the conformations of these bound complexes more precisely.

Discussion

The activation mechanisms by which OPRTase (Victor et al., 1979b) and HGPRTase (Ali & Sloan, 1983) are activated by divalent metal ions have been examined through kinetic analysis of the effects of Mn(II), Mg(II), and Co(II) on these activities. Additionally, the effects of the addition of Zn(II) and Ni(II) on the HGPRTase activity have been characterized (Ali & Sloan, 1986). These studies revealed that divalent metal ions play at least two roles at the active sites of these enzymes. For OPRTase, both the apoenzyme and holoenzyme are active (eq 9) and will bind M(II)–PRibPP, the true sub-

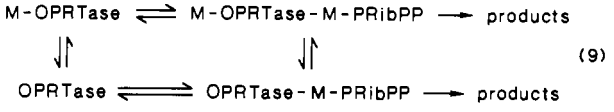

(9)

strate of this reaction. In contrast, only the holoenzyme form of HGPRTase is active and will bind M(II)–PRibPP or individual components of this complex (eq 10). The present

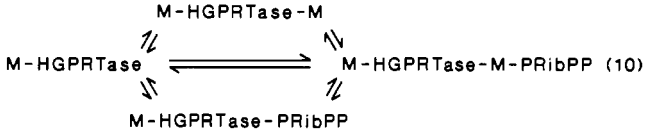

(10)

relaxation rate investigations were successful in revealing the structures of binary complexes of Mn(II)–PRibPP with apo-OPRTase and apo-HGPRTase. The levels of metal ion used in the NMR experiments are well below those required for optimal activity of either enzyme. We speculate that the binding of a second metal ion at these active sites, in addition to providing positive charge for neutralization of the highly negative PRibPP molecule, would coordinate the 5′-phosphate of this substrate and pull this moiety away from the ribose ring, thereby exposing the 1′-ribose carbon for on-line displacement of the pyrophosphate group by purines (HGPRTase) or for displacement/elimination of this group by the enzyme itself (OPRTase). It has been demonstrated by Smithers and O'Sullivan (1982) using ^{31}P NMR that the Mg(II)–PRibPP–Mg(II) complex readily forms in solution at relatively high concentrations of this metal ion and at PRibPP to metal ion concentration ratios near to and beyond those where optimal activation occurs for the OPRTase- and HGPRTase-catalyzed reactions. These researchers determined, as expected, that one of the metal ions is associated with the pyrophosphate group whereas one is associated with the phosphate group.

Our magnetic relaxation studies with Mn(II) of the conformation of PRibPP bound to both OPRTase and HGPRTase have revealed more similarities than differences in the binding site geometry of this substrate. Interestingly, it has been suggested that these enzymes, as well as all other phosphoribosyltransferases, should contain a common domain for PRibPP and that the secondary structure should be similar to the ATP binding sites on several kinases (Argos et al., 1983). In this regard, we have defined structures for PRibPP both on and off OPRTase and HGPRTase that possess "triphosphate" character in the positioning of the phosphate and pyrophosphate groups about the metal ion. This suggests that the initial conformation of PRibPP at the active site may be ATP-like. In order to explore whether any differences exist between the PRibPP–OPRTase and PRibPP–HGPRTase complexes after this initial binding event, we will next examine the effect of optimal Mg(II) concentrations on the NOE of the protons of PRibPP bound to these two enzymes.

Acknowledgments

We acknowledge the contributions of Linda Z. Ali and Robert W. Ashton, who participated in the enzyme purifications and several valuable discussions of the distance calculations presented in this paper.

Registry No. OPRTase, 9030-25-5; HGPRTase, 9016-12-0; PRibPP, 7540-64-9; chromium, 7440-47-3; cobalt, 7440-48-4; manganese, 7439-96-5.

References

Ali, L. Z., & Sloan, D. L. (1982) *J. Biol. Chem. 257*, 1149–1155.
Ali, L. Z., & Sloan, D. L. (1983) *Biochemistry 22*, 3419–3424.
Ali, L. Z., & Sloan, D. L. (1986) *J. Inorg. Biochem. 28*, 407–415.
Argos, P., Hanei, M., Wilson, J. M., & Kelley, W. N. (1983) *J. Biol. Chem. 258*, 6450–6457.
Bloembergen, N. (1957) *J. Chem. Phys. 27*, 572–573.
Ferrin, L. J., & Mildvan, A. S. (1985) *Biochemistry 24*, 6904–6913.
Flaks, J. G. (1963) *Methods Enzymol. 6*, 144–148.
Hill, D. L. (1970) *Biochem. Pharmacol. 19*, 545–557.
Jarori, G. K., Ray, B. D., & Rao, B. D. N. (1985) *Biochemistry 24*, 3487–3494.
Kowalewski, J., Levy, G. C., Johnson, L. F., & Palmer, L. (1977) *J. Magn. Reson. 26*, 533–536.
Luz, Z., & Meiboom, S. (1964) *J. Chem. Phys. 40*, 2686–2692.
Mildvan, A. S., & Cohn, M. (1966) *J. Biol. Chem. 241*, 1178–1193.
Mildvan, A. S., & Cohn, M. (1970) *Adv. Enzymol. Relat. Areas Mol. Biol. 33*, 1–70.
Mildvan, A. S., & Engle, J. (1972) *Methods Enzymol. 26*, 654–682.
Mildvan, A. S., & Grisham, C. M. (1974) *Struct. Bonding (Berlin) 20*, 1–21.
Mildvan, A. S., & Gupta, R. K. (1978) *Methods Enzymol. 49*, 322–359.
Mildvan, A. S., Nowak, T., & Fung, C. H. (1973) *Ann. N.Y. Acad. Sci. 222*, 192–210.
Nowak, T., & Mildvan, A. S. (1972) *Biochemistry 11*, 2819–2828.
Peterson, L. R., & Gupta, R. K. (1979) *Biophys. J. 27*, 1–14.
Rao, B. D. N. (1984) in *Phosphorus-31 NMR, Principles and Application* (Gorenstein, D., Ed.) pp 57–103, Academic, New York.
Ray, W. J., Jr., & Mildvan, A. S. (1970) *Biochemistry 9*, 3886–3894.
Schmidt, R., Weigand, H., & Reichert, U. (1979) *Eur. J. Biochem. 93*, 355–361.
Slater, J. P., Mildvan, A. S., & Loeb, L. A. (1971) *Biochem. Biophys. Res. Commun. 44*, 37–43.
Sloan, D. L. (1984) *Adv. Chromatogr. (N.Y.) 23*, 97–124.
Sloan, D. L., & Mildvan, A. S. (1976) *J. Biol. Chem. 251*, 2412–2420.
Sloan, D. L., Loeb, L. A., Mildvan, A. S., & Feldmann, R. J. (1975) *J. Biol. Chem. 250*, 8913–8919.
Smithers, G. W., & O'Sullivan, W. J. (1982) *J. Biol. Chem. 257*, 6164–6170.

Solomon, I. (1955) *Phys. Rev. 99*, 559–565.
Sundaralingam, M. (1969) *Biopolymers 7*, 821–860.
Syed, D. B., Strauss, R. S., Ashton, R. W., & Sloan, D. L. (1985) *Fed. Proc., Fed. Am. Soc. Exp. Biol. 44*, 672.
Tinkham, M., Weinstein, R., & Kip, A. F. (1951) *Phys. Rev. 84*, 848–849.
Umezu, K., Amaya, T., Yashimoto, A., & Tomita, K. (1971) *J. Biochem. (Tokyo) 70*, 249–269.
Victor, J., Greenberg, L. B., & Sloan, D. L. (1979a) *J. Biol. Chem. 254*, 2647–2655.
Victor, J., Leo-Mensah, A., & Sloan, D. L. (1979b) *Biochemistry 18*, 3597–3604.

NMR Studies of the Interaction of Chromomycin A_3 with Small DNA Duplexes I†

Max A. Keniry,‡ Stephen C. Brown,‡,§ Elisha Berman,‖ and Richard H. Shafer*,‡
Department of Pharmaceutical Chemistry, School of Pharmacy, University of California, San Francisco, California 94143, and Department of Organic Chemistry, The Weizmann Institute of Science, 76100 Rehovot, Israel
Received July 3, 1986; Revised Manuscript Received October 30, 1986

ABSTRACT: ^1H and ^{31}P NMR spectral analysis of a chromomycin/d(ATGCAT)$_2$ complex provides strong evidence for a nonintercalative mode of drug binding. Investigation of the imino proton region of the duplex suggests a protection of one of the two guanine imino protons from fast exchange with the bulk water up to at least 45 °C by the drug. Subsequent one-dimensional nuclear Overhauser enhancement experiments place the exchangeable chromomycin chromophoric hydroxyl proton <0.45 nm from this guanine imino proton and the chromophore 7-methyl <0.45 from the internal thymine 6-proton and/or the guanine 8-proton. ^1H two-dimensional NMR reveals that the duplex retains a right-handed B conformation but there are distortions at the TGC region of one chain and large deviations in the chemical shift of protons relative to the uncomplexed duplex in the other chain in the same TGC region. The data suggest that the chromomycin chromophore is oriented such that the hydrophilic side of the ring system is proximal to the helix center in the major groove near the TG region while the aromatic side of the ring is oriented away from the helix but is partially protected from the solvent by the aliphatic chain, which bends back over the two aromatic protons. Changes in the ^{31}P spectrum of the duplex on binding of the drug are different from the effect of either actinomycin or netropsin on nucleic acid fragments.

Chromomycin and the related antibiotics mithramycin and olivomycin are potent inhibitors of in vitro and in vivo DNA[1]-directed RNA synthesis via complex formation with DNA, in the presence of Mg^{2+} (Miyamoto et al., 1966; Berlin et al., 1966; Bakhaera et al., 1968; Wakisaka et al., 1963; Kersten et al., 1967; Kersten & Kersten, 1974; Slavek & Carter, 1975; Remers, 1979; Gause, 1965). They exhibit antitumor behavior against a variety of experimental tumors, although their potential utility is limited by their toxicity (Gause, 1965) and immunosuppressive properties (Imai et al., 1970; Lvashenko & Kolesnikova, 1965). A detailed three-dimensional picture of the structure of the complex appears essential for elucidating the detailed biological action of this antibiotic. Since both chromomycin and a chromomycin/nucleotide complex have eluded X-ray crystal analysis to this present time, one-dimensional and two-dimensional nuclear magnetic resonance (NMR) techniques become the method of choice for determining these structures.

In the past 2 decades, a variety of techniques has been applied to the binding properties of chromomycin to DNA. There is an absolute requirement for 2-aminopurine residues such as guanine (Ward et al., 1965; Cerami et al., 1967) prompting comparisons with actinomycin. A direct and tight noncovalent binding to guanine-containing DNA is not disputed (Behr & Hartmann, 1965; Kersten, 1965; Cobreros et al., 1982). Helicity in the DNA is a requirement for binding; separated strands show no interaction with chromomycin (Behr et al., 1969). However, the position and mode of the binding remain a matter of controversy. No doubt, the apparent similarity of binding properties with actinomycin (which has been shown to intercalate; Brown et al., 1984) has prompted some to propose an intercalative mode of binding for chromomycin (Behr et al., 1969; Horwitz & McGuire, 1978), but there is evidence to suggest a different mode of binding. Chromomycin does not alter the sedimentation coefficient of normal double-stranded DNA (Cobreros et al., 1982), and unlike actinomycin, it does not induce unwinding and rewinding of the double helix in supercoiled DNA (Waring, 1970). Recent ^{13}C and ^1H NMR studies of drug complexes with fragments of calf thymus DNA, however, produced additional evidence of similarity between the binding of actinomycin and chromomycin and new support for the interca-

† Supported in part by U.S. Public Health Service Grant CA 27343 awarded by the National Cancer Institute, DHHS, and Grant 84-00011 from the U.S.–Israel Binational Science Foundation. This work has benefitted through the use of facilities made available to the School of Pharmacy (NIH Grants RR01668 and RR01695 and NSF Grant DMB8406826).
‡ University of California.
§ Present address: Department of Biology, University of Pennsylvania, Philadelphia, PA 19104.
‖ The Weizmann Institute of Science.

[1] Abbreviations: ACTD, actinomycin D; CRA, chromomycin A_3; COSY, ^1H two-dimensional *J*-correlation NMR; DNA, deoxyribonucleic acid; EGTA, ethylene glycol bis(β-aminoethyl ether)-*N,N,N',N'*-tetraacetic acid; FID, free induction decay; HOHAHA, homonuclear Hartmann–Hahn relayed spectroscopy; HPLC, high-pressure liquid chromatography; NMR, nuclear magnetic resonance; NOE, nuclear Overhauser enhancement; NOESY, ^1H two-dimensional NOE correlation NMR in the pure absorption mode; RNA, ribonucleic acid; 2D, two dimensional.

0006-2960/87/0426-1058$01.50/0